Universiteit Leiden
The Netherlands

Targeting endoglin-expressing regulatory T cells in the tumor microenvironment enhances the effect of PD1 checkpoint inhibitor immunotherapy

Schoonderwoerd, M.J.A.; Koops, M.F.M.; Angela, R.A.; Koolmoes, B.; Toitou, M.; Paauwe, M.; ... ; Hawinkels, L.J.A.C.

Citation
Schoonderwoerd, M. J. A., Koops, M. F. M., Angela, R. A., Koolmoes, B., Toitou, M., Paauwe, M., … Hawinkels, L. J. A. C. (2020). Targeting endoglin-expressing regulatory T cells in the tumor microenvironment enhances the effect of PD1 checkpoint inhibitor immunotherapy. *Clinical Cancer Research*, *26*(14), 3831-3842. doi:10.1158/1078-0432.CCR-19-2889

Version: Publisher's Version
License: Creative Commons CC BY 4.0 license
Downloaded from: https://hdl.handle.net/1887/3181884

Note: To cite this publication please use the final published version (if applicable).

Targeting Endoglin-Expressing Regulatory T Cells in the Tumor Microenvironment Enhances the Effect of PD1 Checkpoint Inhibitor Immunotherapy

Mark J.A. Schoonderwoerd[1], Maaike F.M. Koops[1], Ricardo A. Angela[1], Bryan Koolmoes[1], Melpomeni Toitou[1], Madelon Paauwe[1], Marieke C. Barnhoorn[1], Yingmiao Liu[2], Cornelis F.M. Sier[3], James C.H. Hardwick[1], Andrew B. Nixon[2], Charles P. Theuer[4], Marieke F. Fransen[5], and Lukas J.A.C. Hawinkels[1]

ABSTRACT

Purpose: Endoglin is a coreceptor for TGFβ ligands that is highly expressed on proliferating endothelial cells and other cells in the tumor microenvironment. Clinical studies have noted increased programmed cell death (PD)-1 expression on cytotoxic T cells in the peripheral blood of patients with cancer treated with TRC105, an endoglin-targeting antibody. In this study, we investigated the combination of endoglin antibodies (TRC105 and M1043) with an anti-PD1 antibody.

Experimental Design: The combination anti-endoglin/anti-PD1 antibodies was tested in four preclinical mouse models representing different stages of cancer development. To investigate the underlying mechanism, Fc-receptor–knockout mice were used complemented with depletion of multiple immune subsets in mice. Tumor growth and the composition of immune infiltrate were analyzed by flow cytometry. Finally, human colorectal cancer specimens were analyzed for presence of endoglin-expressing regulatory T cells (Treg).

Results: In all models, the combination of endoglin antibody and PD1 inhibition produced durable tumor responses, leading to complete regressions in 30% to 40% of the mice. These effects were dependent on the presence of Fcγ receptors, indicating the involvement of antibody-dependent cytotoxic responses and the presence of $CD8^+$ cytotoxic T cells and $CD4^+$ Th cells. Interestingly, treatment with the endoglin antibody, TRC105, significantly decreased the number of intratumoral Tregs. Endoglin-expressing Tregs were also detected in human colorectal cancer specimens.

Conclusions: Taken together, these data provide a rationale for combining TRC105 and anti-PD1 therapy and provide additional evidence of endoglin's immunomodulatory role.

Introduction

The tumor microenvironment (TME) is composed mainly of cancer-associated fibroblasts (CAF), infiltrating immune cells, and blood vessels, which are partly enveloped by pericytes. Endothelial cells in the newly formed blood vessels in the TME highly express the TGFβ coreceptor endoglin, which has been correlated with poor prognosis and metastatic disease in many solid tumors (1, 2). Upon stimulation with ligands, including bone morphogenetic protein (BMP) and TGFβ, endoglin promotes endothelial cell proliferation and migration, via signaling through phosphorylation of the SMAD-1 signaling molecule. In previous work, we and others demonstrated that endoglin is also expressed on CAFs, in particular at the invasive margin of colorectal tumors (3) and on mononuclear cells including lymphocytes and activated macrophages (4, 5).

TRC105 (carotuximab, TRACON Pharmaceuticals, Inc.) is a humanized IgG1 endoglin-neutralizing antibody, which has been studied in multiple clinical trials in oncology and age-related macular degeneration. In preclinical cancer models, we and others have shown that treatment with TRC105 inhibits angiogenesis, tumor growth, and metastases (6–10). Notably, TRC105 treatment might engage antibody-dependent cellular cytotoxicity (ADCC; ref. 11) and is more potent in immunocompetent mice compared with immunodeficient mice, indicating the active involvement of the immune system (7). TRC105 binds to human endoglin with high avidity and inhibits BMP9 binding, but binds much less avidly to mouse endoglin, with consequently less inhibition of murine BMP9 binding. Therefore, a mouse-specific endoglin-targeting rat IgG1 antibody, M1043, has been developed for preclinical studies. This antibody efficiently inhibits BMP9-induced endoglin signaling in mice (12).

Program cell death receptor 1 (PD1/CD279) is an immune checkpoint molecule which plays an important role in preventing self-reactive T-cell responses (13). The PD1 ligands PD-L1 and PD-L2 are found on tumor cells, fibroblasts, and myeloid cells (14). Inhibition of PD1 reactivates the tumor immune responses, and PD1 antibodies have been approved for the treatment of melanoma (15), non–small cell lung cancer (16), and renal cell carcinoma (17). In addition, anti-PD1 therapy has been approved for patients with cancer with high microsatellite instability representing the first tissue agnostic companion diagnostic approved by the FDA. In clinical trials, treatment with TRC105 increased PD1 expression on $CD8^+$ T cells in the blood of patients with cancer (18). Because the effects of TRC105 have been

[1]Department of Gastroenterology and Hepatology, Leiden University Medical Center, Leiden, the Netherlands. [2]Department of Medicine, Duke University Medical Center, Durham, North Carolina. [3]Department of Surgery, Leiden University Medical Center, Leiden, the Netherlands. [4]Tracon Pharmaceuticals, San Diego, California. [5]Department of Immunohematology and Blood Transfusion, Leiden University Medical Center, Leiden, the Netherlands.

Note: Supplementary data for this article are available at Clinical Cancer Research Online (http://clincancerres.aacrjournals.org/).

M.F.M. Koops, R.A. Angela, M.F. Fransen, and L.J.A.C. Hawinkels contributed equally to this article.

Corresponding Author: Lukas J.A.C. Hawinkels, Leiden University Medical Center, Building 1, C4-P, P.O. Box 9600, Leiden 2300 RC, the Netherlands. Phone: 31-71-526-6736; Fax: 31-71-524-8115; E-mail: L.J.A.C.Hawinkels@lumc.nl

Clin Cancer Res 2020;26:3831–42

doi: 10.1158/1078-0432.CCR-19-2889

©2020 American Association for Cancer Research.

Downloaded from http://aacrjournals.org/clincancerres/article-pdf/26/14/3831/2062840/3831.pdf by Leiden Uni - WALAEUS LIBRARY user on 01 September 2022

Translational Relevance

Immune checkpoint inhibitors are being successfully used clinically for the treatment of multiple cancer types and are often used in combination with other therapies. In this study we investigated the combination of endoglin targeting using the neutralizing antibody TRC105 with PD1 checkpoint inhibitors in multiple mouse cancer models. Our data show that combined therapy of TRC105 with anti-PD1 shows robust antitumor effects by enhancing antitumor immune responses and targeting of endoglin-expressing regulatory T cells, which were also detected in human colorectal cancer samples. These findings indicate that combined TRC105/anti-PD1 therapy might be a valuable approach for treatment of patients with cancer. Results from a phase Ib dose escalation study of carotuximab (TRC105) in combination with nivolumab (anti-PD1) in patients with metastatic non–small cell lung cancer (NCT03181308) should reveal whether this combination strategy is effective in human patients.

described to be immune dependent and PD1 expression is increased upon TRC105 treatment, we hypothesized that a combination of TRC105 with anti-PD1 antibody therapy might enhance therapeutic responses.

In this study, we evaluated the effects of endoglin-targeting antibodies in combination with a PD1 antibody in mouse models representing different cancer stages. We compared the efficiency and mechanism of antibodies binding to human and mouse endoglin (TCR105 and M1043, respectively), and investigated the effects of combination treatment. Our data show enhanced therapeutic effects when combining endoglin antibodies with PD1 inhibitors, resulting in prolonged antitumor responses, which are dependent on ADCC and $CD8^+$ cytotoxic T cells. Moreover, we present evidence that targeting endoglin-expressing regulatory T cells (Treg) in the TME reactivates the immunosuppressed TME.

Materials and Methods

Cell culture

The C57BL/6 murine colon adenocarcinoma cell line MC38 and a BALB/c CT26, which stably expresses a codon-optimized luciferase construct (3), were routinely cultured in DMEM/F12 Glutamax with 10 mmol/L HEPES, 50μg/mL gentamicin, 100 U/mL penicillin, and 100μg/mL streptomycin (Invitrogen), supplemented with 10% FCS (Gibco, Thermo Fisher Scientific). Cell lines obtained from ATCC were used for 20 passages and were tested directly before *in vivo* use for *Mycoplasma* contamination by PCR analysis.

Mice

In this study, 8 to 10 weeks old male C57BL/6 or BALB/c mice (Jackson Laboratory) were used. Mice were maintained at the central animal facility at the Leiden University Medical Centre (LUMC, Leiden, the Netherlands) under standard conditions. All mice were treated twice a week with intraperitoneal injections of 10 mg/kg bodyweight M1043 or 15 mg/kg bodyweight TRC105 (both kindly supplied by TRACON Pharmaceuticals) or a human IgG control (inVivoMAB, BioXCell). For the combination studies, mice were additionally treated twice a week with either an anti-PD1 (clone J43, 10 mg/kg bodyweight, i.p. injection) or a hamster IgG control (both inVivoMAB, BioXCell). To investigate the Fcγ receptor (FcγR) interactions, we investigated the therapeutic efficacy of TRC105 and TRC105 in combination with PD1 in an FcγRI/II/III/IV-knockout ($FcγR^{KO}$) mice (19) as described above. CD8- and CD4-dependent effects were studied using 200 μg CD8-depleting antibody and 50 μg for CD4 depletion (anti-CD8 Clone 2.42 and anti-CD4 clone GK1.5 in-house production followed by protein G column purification) given 1 day prior to the therapeutic antibodies CD8 and CD4 depletion was checked using flow cytometry of the blood samples on the day of treatment. The depleting antibody was given once a week during the entire experiment.

To investigate the tumor growth and survival, mice were subcutaneously injected with 25×10^4 MC38 or CT26 tumor cells. When palpable tumors were present, treatment was started as described above and tumor volume was assessed by caliper measurement. Mice were sacrificed when tumors reached 1,500 mm^3. To investigate changes in the tumor immune infiltrate a short-term experiment was performed. Mice were subcutaneously injected with 25×10^4 tumor cells and when tumors were $5 \times 5 \times 5$ mm therapy was started. Ten days after starting of treatment, when tumor sizes were still comparable, mice were sacrificed and after a cardiac injection with 2 mmol/L EDTA (Merck), to eliminate the blood from the vessels, the tumors were collected and processed for histology, flow cytometry, and RNA and protein isolation. For the M1043 studies in subcutaneous MC38 mice a total of 40 female 6- to 8-week-old C57BL/6J mice were inoculated subcutaneously with 2.5×10^5 CEA2-expressing MC38 colon carcinoma cells (20). Once tumors reached 100 mm^3, mice were randomized into four treatment groups: (i) isotype control (rat IgG2a, clone 2A3, catalog no. BE0089, BioXCell); (ii) 5 mg/kg M1043 (provided by TRACON Pharmaceuticals); (iii) anti-mouse PD1 antibody (RMP1-14, catalog no. BE0146, BioXCell) at fixed dose of 150 μg per mouse; and (iv) combination of M1043 and anti-PD1 antibodies at the aforementioned doses. Drugs were injected intraperitoneally every 2 days and tumor sizes monitored. When tumors reached 2,000 mm^3, mice were sacrificed according to the institutional animal use guidelines (Duke University Durham, NC).

For imaging, mice were injected intravenously with 0.1 mg TRC105 labeled with a near-infrared fluorescent dye 800CW according to the manufacturer (LI-COR Biosciences). Mice were imaged using the Pearl Impulse Small Animal Imager (LI-COR Biosciences) 24 and 48 hours after injection, after which mice were sacrificed. Finally, tumors were also imaged *ex vivo*.

For the orthotopic implantation, subcutaneous tumors were grown and upon reaching 0.5 cm^3 mice were sacrificed, and the donor tumors were divided in 1–2 mm^3 pieces. These pieces were transplanted to the caecum wall of recipient mice (21). In short, mice were sedated using isoflurane followed by a small incision in the center of the abdomen. The caecum was isolated and a small piece of tumor ($1 \times 1 \times 1$ mm) was attached to the caecal wall, followed by the closure of the peritoneal wall and skin. Bioluminescent imaging was performed as described before. In short, mice received an intraperitoneal injection with 100 mg/kg luciferin (D-luciferin sodium salt, Synchem) and were subsequently imaged on the IVIS Lumina-II (Perkin Elmer) signal. The signal was quantified using the living image software. Eight days after transplantation, mice were randomized on the basis of equal bioluminescent signal after which treatment was started. Thirty-six days after transplantation mice were imaged, sacrificed, and the tumor volume was measured using a caliper.

To investigate early stages of cancer development, the azoxymethane (AOM) dextran sulphate sodium (DSS) colitis-associated cancer model was used. Wild-type C57/Bl6 jico mice received one intraperitoneal injection with 10 mg/kg azoxymethane (Sigma), which

Downloaded from http://aacrjournals.org/clincancerres/article-pdf/26/14/3831/2062840/3831.pdf by Leiden Uni - WALAEUS LIBRARY user on 01 September 2022

induces aberrant DNA methylations in the colon and liver (22). To accelerate tumor formation, mice were subsequently exposed to three, 7-day cycles of 1.5% DSS (MP Biomedicals) supplied in the drinking water with 2-week intervals. Mouse weights were monitored every other day. In previous studies we observed small colonic lesions 48 days after azoxymethane injections. Therefore, therapy was started at this timepoint. At the end of the experiment (84 days), mice were sacrificed by cervical dislocation and colons and livers were obtained. The number of colonic lesions was counted and one lesion per mouse was used for flow cytometric analysis. The remaining material was fixed in 4% buffered formaldehyde (Added Pharma) and embedded in paraffin (Leica Biosystems).

Flow cytometry

Tumors were mechanically disrupted and incubated for 15 minutes at 37°C in DMEM containing 1 mg/mL liberase TL (Roche). Single-cell suspensions were prepared by mincing the tumors through a 70-μm cell strainer (BD Bioscience). For cell surface staining, cells were resuspended in FACS buffer (PBS + 0.5% BSA, Sigma) + 0.05% sodium azide (pharmacy, LUMC, Leiden, the Netherlands). Cells were stained with Life death UV marker, specific antibodies indicated in Supplementary Tables S1 (mouse) and S2 (human) or MC38-specific tetramers (kindly provided by Kees Franken, Department of Immunohematology and Blood Transfusion, LUMC, Leiden, the Netherlands) for 1 hour. After incubation, cells were washed 3 times with FACS buffer and analyzed on an LSRII (BD Bioscience). For the FoxP3 staining, the eBioscience Foxp3/Transcription Factor staining buffer set was used according to the one-step protocol for intranuclear proteins. Data analyses were performed using FlowJo 10.0.6 (FlowJo, data analysis software).

Histology

Four-micrometers sequential sections were deparaffinized and stained with hematoxylin and eosin (H&E) or processed for IHC as described before (10). In short, sections were deparaffinized and blocked in 0.3% hydrogen peroxidase (H_2O_2, Merck) in methanol for 20 minutes. Next, slides were rehydrated, and antigen retrieval was performed by boiling in 0.01 mol/L sodium citrate pH 6.0 for 10 minutes. Slides were washed and incubated with primary antibodies against CD31 (1:1,600, Santa Cruz Biotechnology), α-smooth muscle actin (SMA; 1:1,600, Progen), endoglin (1:100, R&D Systems), and Foxp3 (1:25, Thermo Fisher Scientific) diluted in 1% PBS/BSA overnight at room temperature in a humidified box. The next day, slides were incubated with appropriate biotinylated secondary antibodies (Dako) or anti-Goat-alexa488 (Abcam) and anti-Rat-alexa568 (Invitrogen). For immunofluorescence staining, slides were mounted with prolong gold anti fade (Thermo Fisher Scientific) including DAPI. For IHC, slides were incubated for 30 minutes at room temperature using Vectastain complex (Vector Laboratories). Staining was visualized with the DAB + reagent (Dako) for 10 minutes. Nuclei were counterstained with Mayer's Hematoxylin (Merck) and slides were rinsed in tap water, dehydrated, and mounted using Entellan (Merck). Finally, pictures were taken with an Olympus BX51 Light Microscope equipped with an Olympus DP25 camera using the program CellSense and analyzed using ImageJ. For confocal microscopy, LICA SP8 Lightning was used and pictures were processed using LICA LAS-X software.

Statistical analysis

Statistical analysis was performed using GraphPad/Prism software, version 7.0 (GraphPad Prism Software, Inc.). All data are presented as mean ± SD unless otherwise indicated. Differences in survival were assessed by the log-rank/Mantel–Cox test. For all others, when normally distributed, Student *t* test and ANOVA or Kruskal–Wallis (nonparametric) test were used to test for significant differences, as indicated in the figure legends. $P < 0.05$ was considered statistically significant.

Ethical approvals

All experiments using human material were performed according to the code of conduct for responsible use of human tissue and medical research as drawn up by the federation of the Dutch medical societies in 2011, guidelines of Medical Ethical Committee of the LUMC (Leiden, the Netherlands), and conducted in accordance to the declaration of Helsinki.

All animal experiments were approved by the national Dutch animal ethics committee under project license number AVD116002017858 and AVD11600201571 and in accordance with the rules and regulation of the animal welfare body of the LUMC (Leiden, the Netherlands). Animal experiments conducted at Duke University (Durham, NC) were performed in the Duke Preclinical Translational Research Unit in accordance with the Institutional Animal Care and Use Committee of Duke University and Duke University Medical Center (Durham, NC).

Results

Combined endoglin/PD1 targeting reduces tumor burden in a chemically induced colorectal cancer model

To investigate whether endoglin targeting can decrease tumor burden in early-stage colorectal tumor development and whether therapeutic effects can be enhanced together with checkpoint inhibition, we employed an azoxymethane DSS colitis-associated cancer model. These mice show high-grade adenomas with dysplasia, but without invasion through the basement membrane (Supplementary Fig. S1A–S1C). Mice were either treated with endoglin antibody (TRC105 or M1043) and/or PD1 antibody or appropriate IgG controls starting at day 48 after azoxymethane injection. At the end of the experiment (day 84) mice were sacrificed and the number of colonic lesions was counted. Treatment with TRC105 significantly reduced the number of lesions compared with control, which was further reduced by combination with a PD1 antibody (**Fig. 1A** and **B**), although the combination reached no statistical significance ($P = 0.11$) over TRC105 monotherapy. Furthermore, the size of the remaining lesions was also significantly reduced by TRC105 and the TRC105/PD1 combination compared with IgG controls (**Fig. 1C**). Because TRC105 binds to mouse endoglin with low affinity, we also used M1043, a specific mouse endoglin–neutralizing antibody. In contrast to TRC105, M1043 monotherapy did not reduce the number of lesions in this experiment, although the combination with PD1 was highly effective in reducing the lesion count and size (**Fig. 1D–F**). Taken together, these data show that targeting endoglin by using TRC105 can reduce tumor burden in an early-stage tumor model and that these effects can be enhanced by combining endoglin and PD1-targeting antibodies.

TRC105/anti-PD1 therapy inhibits orthotopic MC38 tumor growth

To investigate the effects of combination therapy in a more advanced cancer model, we used a MC38 syngeneic orthotopic transplantation model. In short, part of a subcutaneously grown MC38 tumor, expressing codon-optimized luciferase, was transplanted onto

Downloaded from http://aacrjournals.org/clincancerres/article-pdf/26/14/3831/2062840/3831.pdf by Leiden Uni - WALAEUS LIBRARY user on 01 September 2022

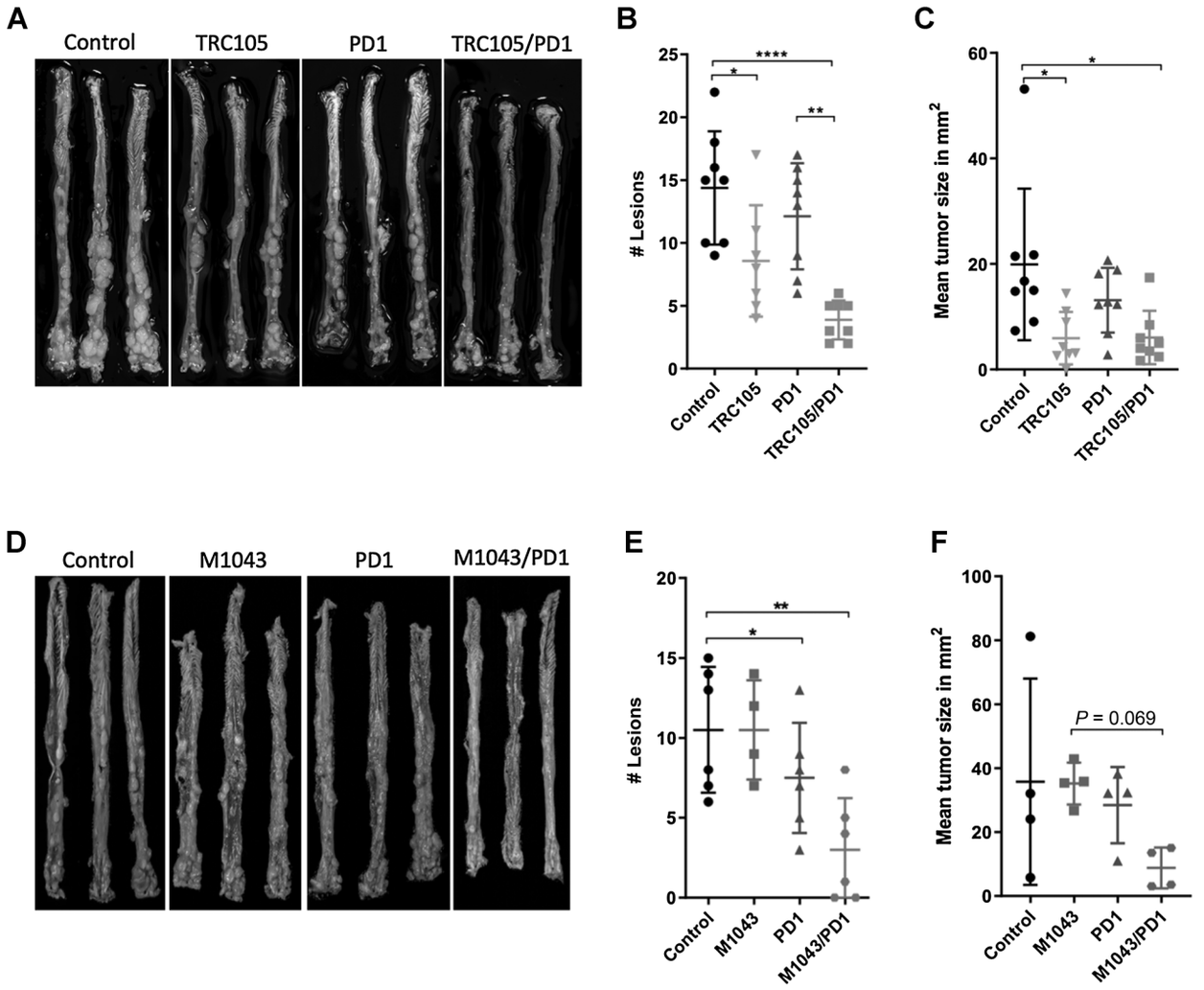

Figure 1.

Combined endoglin/PD1 targeting reduces tumor burden in a chemically induced colon cancer model. Azoxymethane/DSS model to study early colon tumor development. From day 48 onward mice were treated twice weekly with anti-endoglin antibodies or control IgG and twice a week with anti-PD1 or IgG control until day 84 when mice were sacrificed. **A,** Images obtained from the mouse colon at the end of the experiment (84 days) showing multiple lesions in the distal colon. **B,** Quantification of the number of colonic lesions upon treatment with control IgG, anti-PD1, anti-endoglin (TRC105), and the TRC105/PD1 combination. Combination-treated mice show significantly reduced tumor formation compared with monotherapy and IgG controls (one-way ANOVA). **C,** Tumor volume measurements showing significantly smaller tumors in the combination-treated mice (Kruskal–Wallis test for multiple comparison). **D,** Images obtained from the distal mouse colon at the end of the experiment showing multiple lesions. **E,** Quantification of the number of lesions showing a significant decrease in the combination group (M1043/PD1) compared with the IgG controls (one-way ANOVA). **F,** Tumor volume measurement of the colonic lesions (Kruskal–Wallis test for multiple comparison). Data shown are representative from two or more independent experiments with 6–8 mice per group (*, $P \leq 0.05$; **, $P < 0.01$; ****, $P < 0.0001$).

the caecal wall of recipient mice (Supplementary Fig. S2A). Bioluminescent imaging was performed at day 8 after tumor transplantation, after which mice were allocated into treatment groups based on equal bioluminescent signal (Supplementary Fig. S2B). Tumor-specific T-cell effects were assessed at day 17 (9 days after start treatment) by flow cytometry for the MC38-specific neoepitopes ADPGK and DPAGT-1 tetramers (ref. 23; gating strategy in Supplementary Fig. S2C). $CD8^+$ DPAGT-1–positive cells increased slightly in the TRC105-, PD1-, and combination-treated mice compared with controls. M1043 alone did not induce tumor-specific T cells (Supplementary Fig. S2D). A similar trend was present in ADPGK-recognizing CD8 T cells, but did not reach statistical significance (Supplementary Fig. S2E). At the end of the experiment (36 days after tumor transplantation), mice were sacrificed and the tumor volume was determined by caliper measurements. In contrast to M1043, TRC105 and PD1 antibody monotherapy and the combination of M1043 and PD1 antibody treatment resulted in reduced tumor volume compared with control IgG. Strikingly, the combination of TRC105 and PD1 antibody resulted in a more profound reduction of the tumor volume by bioluminescent imaging and caliper measurements (**Fig. 2A** and **B**). Remaining tumors were processed for histologic analysis and stained for H&E, the pan-endothelial marker CD31 (**Fig. 2A**, middle) and endoglin (**Fig. 2A**, right), using an antibody recognizing a non-overlapping endoglin epitope. No significant differences were detected

Downloaded from http://aacrjournals.org/clincancerres/article-pdf/26/14/3831/2062840/3831.pdf by Leiden Uni - WALAEUS LIBRARY user on 01 September 2022

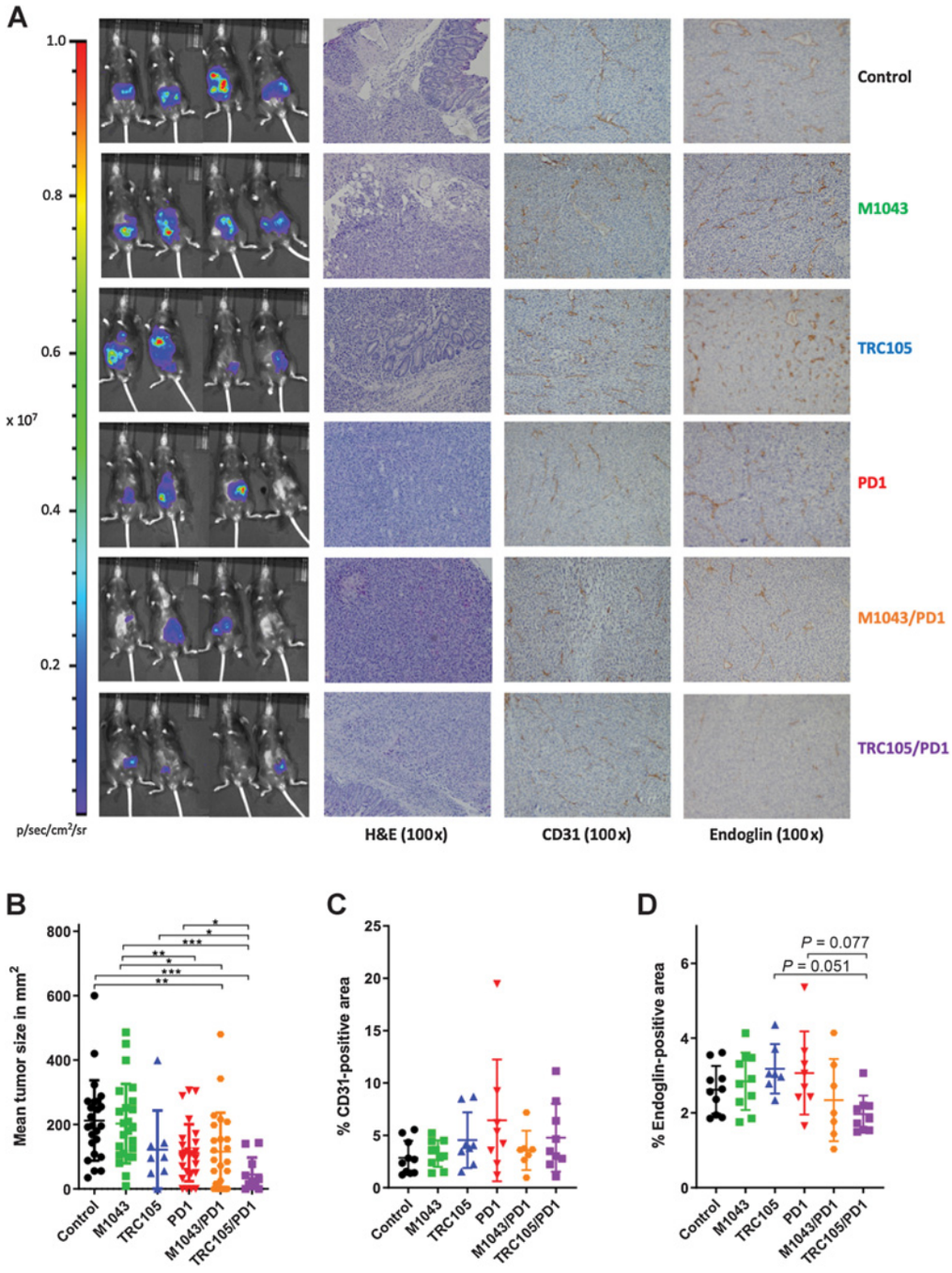

Figure 2.

Endoglin/PD1 therapy inhibits orthotopic tumor growth. Tumors were orthotopically transplanted in recipient mice and after engraftment and randomization, mice were treated twice a week with anti-endoglin or control IgG and twice a week with anti-PD1 or IgG control. **A,** Bioluminescent imaging (left) at the end of the experiment showing antitumor responses. IHC analysis for H&E, CD31, and endoglin (right). **B,** Quantification of the tumor volume at the end of the experiment showing significantly smaller tumors upon combination therapy, especially in the TRC105/PD1 group. Data are from two independent experiments with 8–20 mice per group (one-way ANOVA). **C,** Quantification of tumor CD31 staining showing no significant difference in the number of $CD31^+$ cells (Kruskal–Wallis test for multiple comparison). **D,** Quantification of intratumoral endoglin staining showing no significant differences between treatment groups. Quantifications are from at least two independent experiments (one-way ANOVA; *, $P \leq 0.05$; **, $P < 0.01$; ***, $P < 0.001$).

Downloaded from http://aacrjournals.org/clincancerres/article-pdf/26/14/3831/2062840/3831.pdf by Leiden Uni - WALAEUS LIBRARY user on 01 September 2022

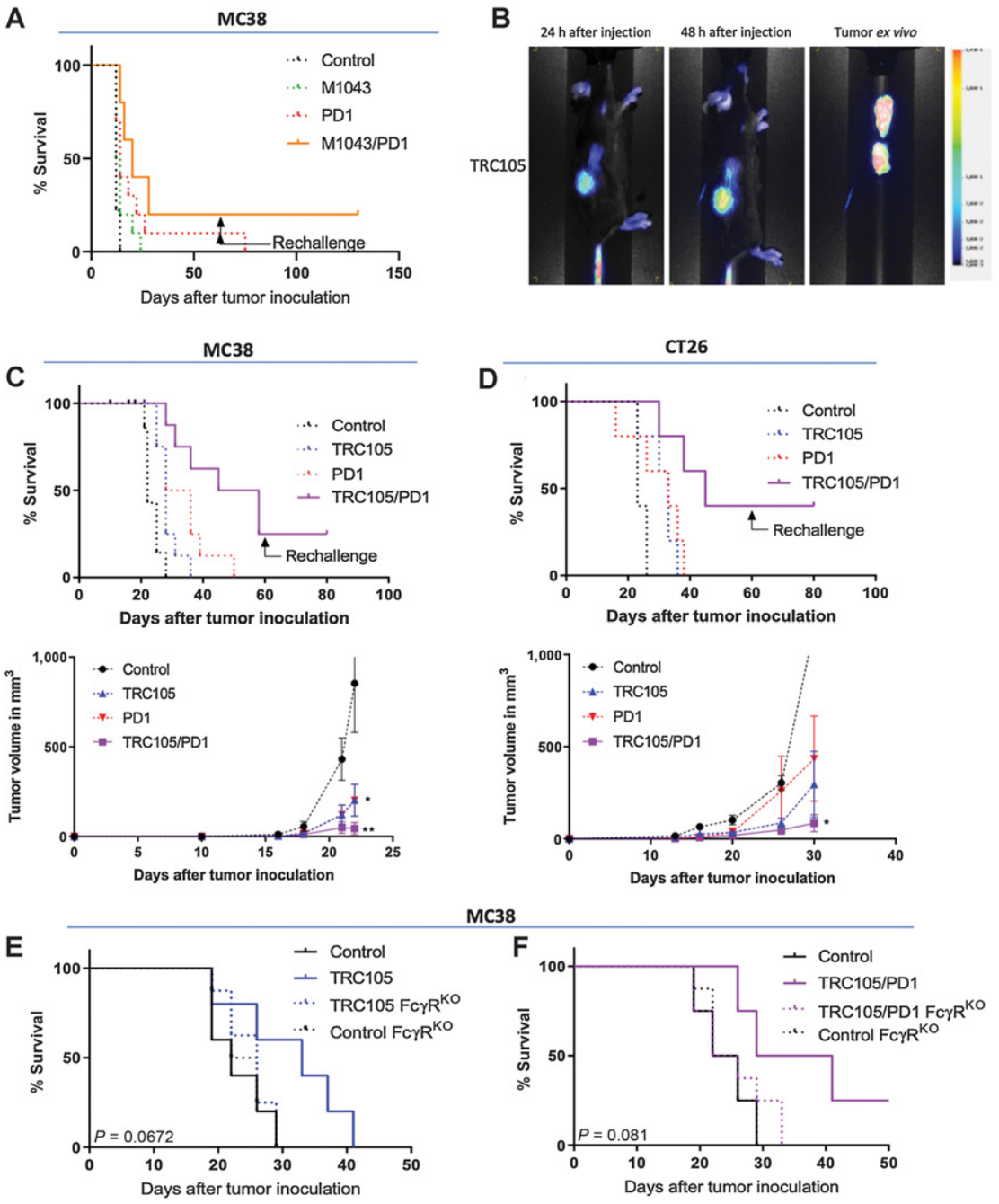

Figure 3.

TRC105/PD1 therapy efficiently reduces tumor growth, induces memory T-cell responses, and is dependent on FcγR expression. When tumors were palpable mice were treated twice a week with anti-endoglin or control IgG and twice a week with anti-PD1 or IgG control. **A,** A combination of M1043 and PD1 results in significantly improved mouse survival and induced memory T-cell responses, because rechallenge with tumor cells does not result in tumor outgrowth. **B,** Intravenously administered CW800-labeled TRC105 shows high tumor accumulation in subcutaneous MC38 tumors (representative image from 2 mice). Combination treatment with TRC105/PD1 significantly increases survival of mice bearing MC38 ($n = 7$–8 mice per group; **C**) or CT26 subcutaneous tumors ($n = 5$ mice per group; **D**). Therapeutic effects of TRC105 (**E**) or combination therapy (**F**) are diminished in a FcγR^{KO} mouse, indicating the involvement of ADCC ($n = 5$–8 mice per group). Statistical analysis includes log-rank/Mantel–Cox test for survival analyses, one-way ANOVA for multiple comparison on day 22 for **C** and day 30 for **D** (*, $P \leq 0.05$; **, $P < 0.01$).

Downloaded from http://aacrjournals.org/clincancerres/article-pdf/26/14/3831/2062840/3831.pdf by Leiden Uni - WALAEUS LIBRARY user on 01 September 2022

in the number of CD31 or endoglin-expressing blood vessels (**Fig. 2C** and **D**) in the remaining tumors. Of note, vessel density could not be assessed in mice with complete tumor regressions and differences in tumor size were not considered in the analysis. Combined, these data indicate that TRC105/PD1 antibody therapy induced marked antitumor responses in an orthotopic MC38 colon cancer model and TRC105 seemed more effective in tumor inhibition compared with M1043 therapy.

TCR105/PD1 therapy efficiently reduces tumor growth and induces memory antitumor responses

To assess the immune responses in more detail, we evaluated the therapeutic effectivity of the mouse endoglin antibody M1043 with PD1 antibody in a subcutaneous MC38 model. A significant delay in tumor outgrowth was observed in the combination therapy–treated mice and resulting complete tumor regression in 20% of the mice in the combination therapy group (**Fig. 3A**; Supplementary Fig. S3A). Given the fact that TRC105 binds murine endoglin with lower avidity, we confirmed that TRC105 can still bind to mouse endoglin and accumulates in subcutaneous mouse tumors. Therefore, we labeled TRC105 with the near-infrared dye CW800. Upon intravenous injection in mice bearing subcutaneous MC38 tumors, tumor accumulation of TRC105 was observed 24 and 48 hours after injection as well as *ex vivo* (**Fig. 3B**).

The subcutaneous MC38 model was used to directly compare the efficiency of M1043 and TRC105 versus an isotype control. These data demonstrate significantly more therapeutic efficacy of TRC105 compared with M1043 (Supplementary Fig. S3B). Therefore, we focused further studies on TRC105/PD1 only. The therapeutic benefit of TRC105/PD1 antibody therapy was assessed in MC38 and CT26 subcutaneous tumor models in C57BL/6 and Balb/c mice, respectively. TRC105 or PD1 antibody monotherapy delayed tumor growth and prolonged survival, but effects were more pronounced in animals who received TRC105/PD1 combination therapy in both the MC38 (**Fig. 3C**) and CT26 model (**Fig. 3D**). Complete tumor responses were observed in 30%–40% of the mice in both models. To investigate memory antitumor responses, the surviving, tumor-free mice were injected again with 2.5×10^5 MC38 or 2.5×10^5 CT26 cells 60 days after the initial tumor cell injection. Importantly, no tumor outgrowth was observed after rechallenge with tumor cells, implying that a memory antitumor response was induced. Our data show that combined TRC105/PD1 antibody therapy delays tumor growth compared with either antibody alone, induces complete and sustained regression in both the MC38 and CT26 subcutaneous tumor models, and prevents tumor growth after rechallenge with tumor cells.

TRC105/PD1 antibody therapeutic effects are ADCC dependent

We next investigated the underlying mechanism for the activity of the TRC105/PD1 antibody combination. TRC105 can mediate ADCC, which requires binding to Fc receptors. We therefore investigated whether the TRC105 and TRC105/PD1 antibody effects were dependent on Fc receptor binding in $Fc\gamma R^{KO}$ mice. MC38 bearing C57Bl6 and $Fc\gamma R^{KO}$ mice injected with human IgG showed similar tumor outgrowth and survival (Supplementary Fig. S3C). Notably, the activity of TRC105 and TRC105/PD1 combination therapy was completely abolished in $Fc\gamma R^{KO}$ mice (**Fig. 3E** and **F**) indicating that the therapeutic effects of TRC105 and the TRC105/PD1 combination are dependent on FcγR binding *in vivo*.

TRC105/PD1 therapy requires T-cell infiltration and activity

Next, we assessed changes in immune cell infiltrate upon combination treatment. Subcutaneous MC38 tumors of similar size (Supplementary Fig. S4A), 9 days after start of treatment, were evaluated to exclude potential effects of tumor volume on the composition of the immune infiltrate. IHC showed decreased numbers of $Ki67^+$ proliferating cells, accompanied by increased numbers of apoptotic, cleaved caspase-3–positive cells (Supplementary Fig. S4B), indicating antitumor responses. The number of endoglin-positive blood vessels was unaffected at this timepoint (Supplementary Fig. S4C). Treatment with TRC105 or the combination of TRC105/PD1 antibody increased the number of intratumoral $CD8^+$ T cells (**Fig. 4A**). Moreover, we observed a significant increase in the number of activated, granzyme $B^+/CD8^+$ T cells upon TRC105 or PD1 or TRC105/PD1 antibody combination therapy in the circulation (**Fig. 4B**). Activation of T cells was further confirmed by mRNA expression analysis of the tumor tissue, showing that granzyme B mRNA expression was particularly increased following TRC105/PD1 antibody combination treatment (**Fig. 4C** and **D**). Increased numbers of tumor-infiltrating $CD8^+$ T cells was confirmed by IHC analysis (**Fig. 4E**). Protein levels of VEGF, INFγ, and TGFβ-1 within the tumor lysates did not differ, although levels varied considerably between and within groups (Supplementary Fig. S4E). Taken together, these data indicate that an increased number of $CD8^+$ T cells were recruited and activated upon TRC105/PD1 combination therapy.

To further investigate whether $CD8^+$ T cells are instrumental for the therapeutic responses, MC38 cells were subcutaneously injected in mice and a $CD8^+$-depleting antibody was given before the initiation of TRC105 or TRC105/PD1 antibody treatment. This resulted in a significantly reduced number of circulating $CD8^+$ T cells (Supplementary Fig. S4F) in these groups. In T-cell–depleted mice, therapeutic responses induced by TRC105 or TRC105/PD1 antibody combination were abolished compared with control IgG–treated mice (**Fig. 4F** and **G**). These data suggest that the therapeutic effect of combination therapy is dependent on the activity of $CD8^+$ T cells and involves their recruitment and activation.

Targeting of FOXP3 immune subsets by endoglin-targeted therapy

On the ninth day, subcutaneous MC38 tumor experiments anti-endoglin therapy did not cause significant differences in the number of peripheral blood $Treg^{CD4+CD25+Foxp3+}$cells pre- and posttreatment or between the treatment groups (**Fig. 5A**). However, we observed a significantly decreased percentage of Tregs in the tumor in the TRC105- and TRC105/PD1 antibody–treated mice, compared with the control IgG and PD1 antibody monotherapy–treated mice (**Fig. 5B**). Moreover, the $CD8^+$/Treg ratio significantly increased to a more beneficial ratio to reach antitumor effects in the combination therapy–treated mice (**Fig. 5C**). A striking increase in endoglin expression on tumor-localized Tregs was present, compared with circulating Tregs in these mice (**Fig. 5D**). Endoglin expression was present only on a subpopulation of Tregs within the tumor and not on conventional $CD4^+$ T cells (**Fig. 5E**). Treatment with TRC105 significantly reduced the number of intratumoral $CD25^+/Foxp3^+$ cells (**Fig. 5F**).

To further investigate the targeting of $Foxp3^+$ Tregs we depleted $CD4^+$ cells, compromising the $Foxp3^+$ population. MC38 cells were subcutaneously injected in mice and a $CD4^+$-depleting antibody was given before the initiation of TRC105 treatment. This resulted in a loss of circulating $CD4^+$ T cells (Supplementary Fig. S5C) in the depleted groups. Mice not showing $CD4^+$ cell depletion (indicated in red) were

Downloaded from http://aacrjournals.org/clincancerres/article-pdf/26/14/3831/2062840/3831.pdf by Leiden Uni - WALAEUS LIBRARY user on 01 September 2022

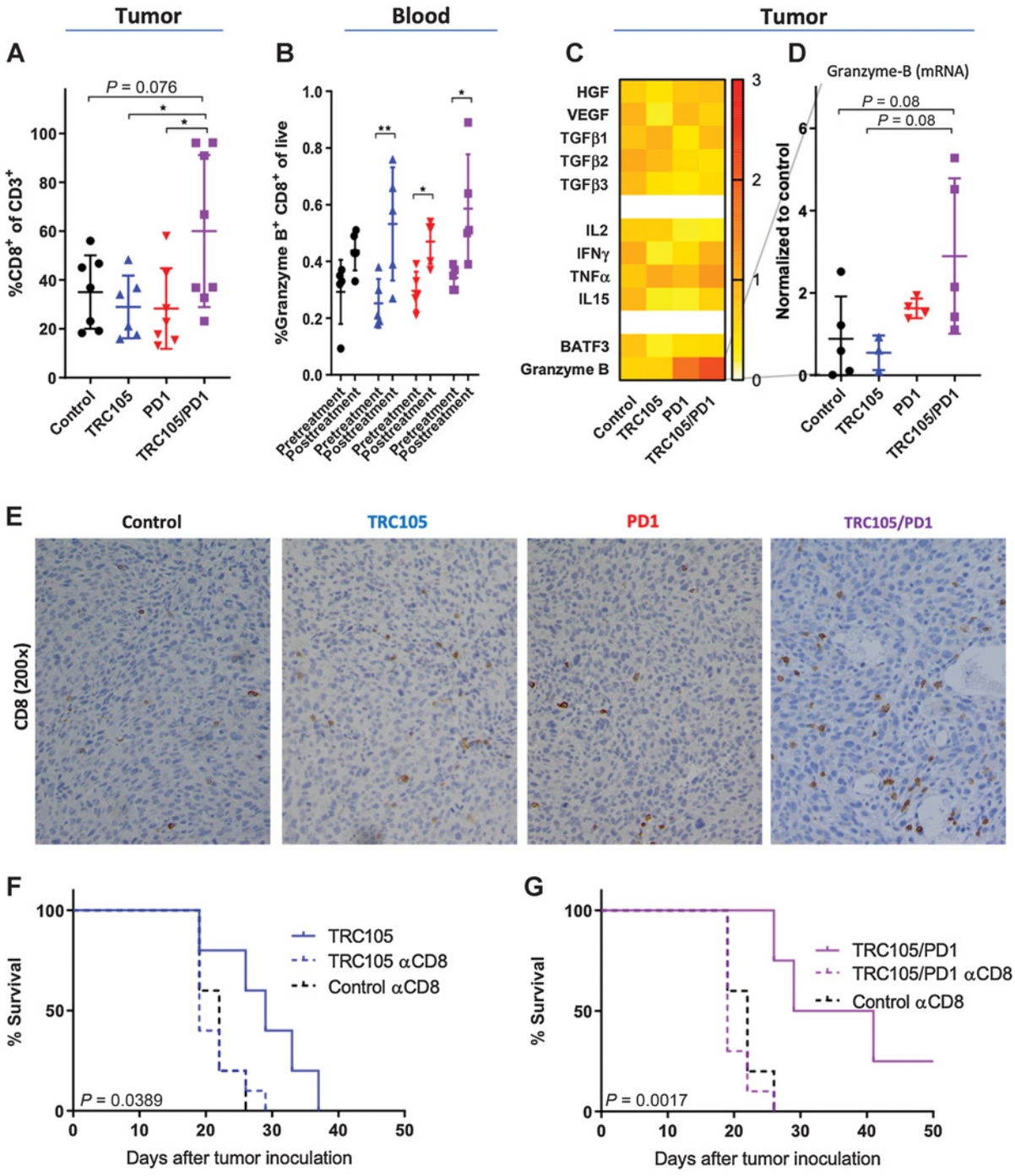

Figure 4.

TRC105/PD1 therapy requires CD8$^+$ T-cell infiltration. When tumors were palpable mice were treated twice a week with anti-endoglin or control IgG and twice a week with anti-PD1 or IgG control. After 9 days of treatment, mice were sacrificed and the immune infiltrate was examined. **A,** Upon treatment with TRC105/PD1 combination therapy the percentage of intratumoral CD8$^+$ T cells is increased (mean of two independent experiments, $n = 4$ mice per group per experiment, one-way ANOVA). **B,** Increased number of circulating granzyme B$^+$ CD8$^+$ T cells posttreatment (n = 3–5 mice per group, paired t test). **C,** Heatmap showing mRNA expression of growth factors and genes involved in immune regulation, normalized to control IgG–treated mice ($n = 3$–5 mice per group). **D,** Increased granzyme B expression within the tumor in combination therapy–treated mice is observed. **E,** Immunostaining revealing increased CD8$^+$ T cells throughout the tumors upon treatment with TRC105/PD1 (one-way ANOVA). The therapeutic effects of TRC105 monotherapy (**F**) and combination therapy (**G**) were completely dependent on CD8$^+$ T cells [n = 5 (control)–10 (CD8 depleted) mice per group, log-rank/Mantel–Cox test; *, $P \leq 0.05$; **, $P < 0.01$].

Downloaded from http://aacrjournals.org/clincancerres/article-pdf/26/14/3831/2062840/3831.pdf by Leiden Uni - WALAEUS LIBRARY user on 01 September 2022

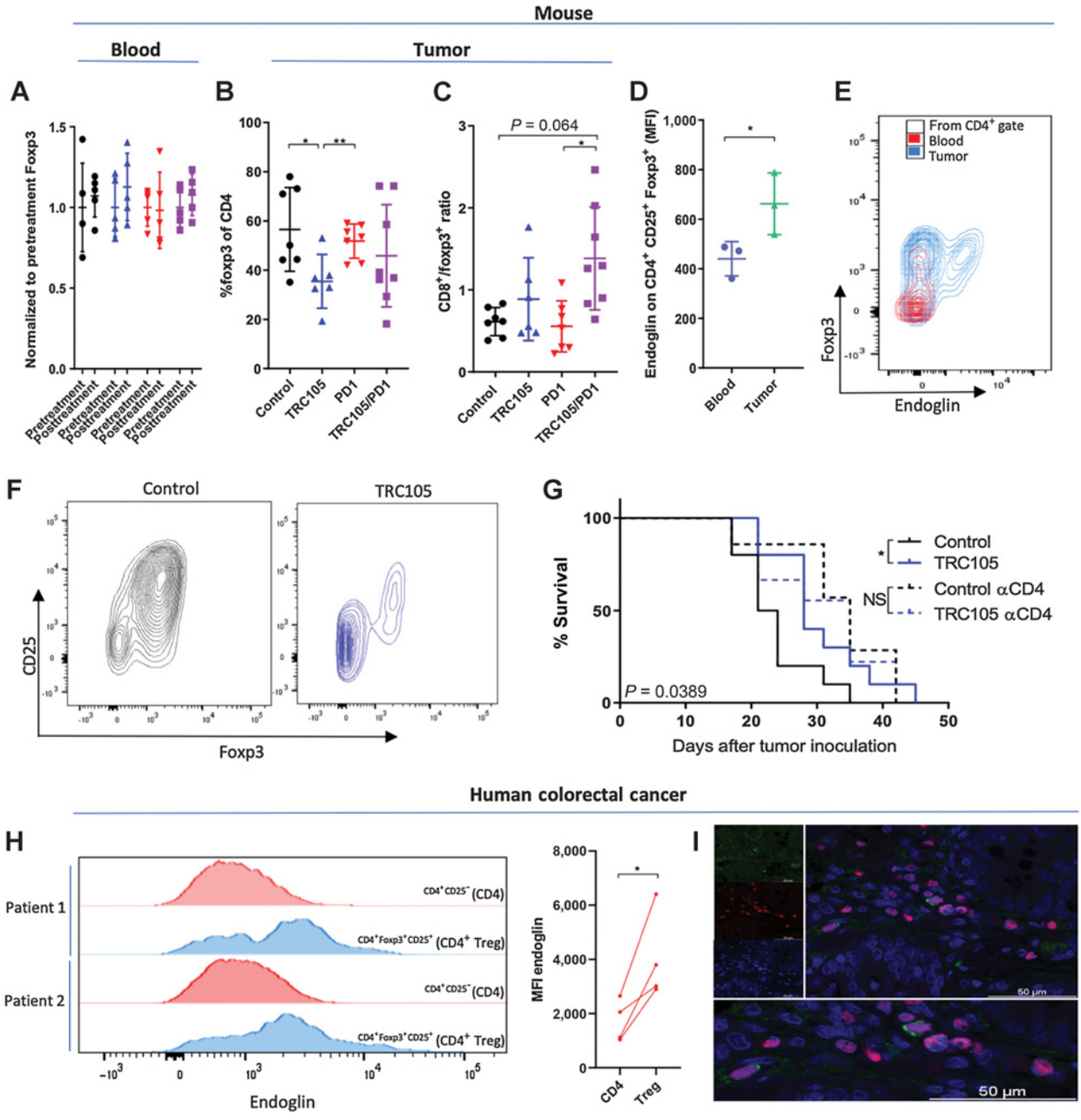

Figure 5.

Endoglin-expressing FoxP3 cells are detected intratumorally and are targeted by anti-endoglin therapy. **A,** The number of FoxP3 cells in the circulation of tumor-bearing mice did not change pre- and posttreatment ($n = 5$ mice per group, paired t test). A significant decrease in intratumoral Tregs ($FoxP3^+CD25^+CD4^+$) was observed (one-way ANOVA; **B**) resulting in increased CD8/FoxP3 tumor ratios (**C,** mean of two independent experiments, $n = 4$ mice per group per experiment, Kruskal-Wallis test for multiple comparison). **D** and **E,** FACS analysis revealed higher endoglin expression on intratumoral FoxP3 cells compared with circulating FoxP3 cells from the same mouse [mean fluorescence intensity (MFI), $n = 3$ mice per group, t test]. **F,** Flow cytometry plot of TRC105-treated MC38 tumors showing a decrease in $CD25^+/Foxp3^+$ cells upon TRC105 treatment. **G,** TRC105 significantly enhances survival of mice bearing MC38 tumors ($P = 0.039$), which is lost upon depletion of $CD4^+$ cells ($P = 0.039$ vs. $P = 0.37$, respectively, $n = 7$–10 mice per group, log-rank/Mantel–Cox test). **H,** In human colorectal cancer samples, endoglin expression on intratumoral Tregs was observed by flow cytometry analysis (representative image from $n = 4$ patients, paired t test). **I,** IHC analysis shows colocalization of endoglin (green) with FoxP3 (red) in a subset of FoxP3 cells in human colorectal cancer tissues (representative image from $n = 4$ patients; *, $P \leq 0.05$; **, $P < 0.01$; NS, not significant).

Downloaded from http://aacrjournals.org/clincancerres/article-pdf/26/14/3831/2062840/3831.pdf by Leiden Uni - WALAEUS LIBRARY user on 01 September 2022

excluded from the experiment. In control mice, TRC105 effectively delayed tumor growth ($P = 0.039$) as shown before. However, the therapeutic effects of TRC105 are lost once the $CD4^+$ T cells were depleted (**Fig. 5G**; $P = 0.37$). These data suggest that therapeutic TRC105 effects are CD4 cell–dependent and most probably involve targeting endoglin-expressing $Foxp3^+/CD4^+$ cells.

Finally to illustrate the potential translational relevance of our findings, we investigated whether endoglin is also expressed on Tregs in a limited number of human colorectal cancer tissues by using flow cytometry. High endoglin expression was seen on a subset of $Tregs^{CD4+CD25+Foxp3+}$ compared with the $CD4+^{CD25\text{-}Foxp3-}$ population within the tumor (**Fig. 5H**). To confirm our flow cytometry findings, we performed immunofluorescence double staining for endoglin and Foxp3 on colorectal cancer tissue sections (**Fig. 5I**). These data revealed high endoglin expression of a subset of intratumoral Tregs. Taken together, our data confirm that a subset of Foxp3 cells coexpress endoglin in mouse colorectal tumors and can also be detected in human colorectal cancer.

Discussion

In this study, we demonstrated that combined therapy with anti-endoglin and anti-PD1 antibodies significantly increases the therapeutic efficacy in several preclinical cancer models, including subcutaneous, orthotopic, and chemically induced colorectal cancer models. The endoglin antibody TRC105 acted principally via immune-dependent mechanisms, where both $CD8^+$ T cells as well as Fc receptors played instrumental roles in the therapeutic response. In addition, we identified endoglin-expressing Tregs in mouse and human colorectal cancer tissue, which also seem to be targeted by TRC105, as the effects are lost when $CD4^+$ cells are depleted.

TRC105 was initially described in the late 1990s (8, 9), and subsequently has been studied in phase II and phase III clinical trials. Because high endoglin expression has been reported on angiogenic endothelial cells and endothelial endoglin expression has been linked to disease progression and prognosis (2), targeting endoglin seems a logical therapeutic approach in solid tumors. Indeed, we and others have shown that anti-endoglin therapy inhibits tumor growth and metastasis formation in various cancer models (6, 8–10, 24). Furthermore, targeting the VEGF pathway activates alternative pathways, of which endoglin has been frequently reported (10, 25–27).

It was surprising that M1043 was less effective in reducing tumor growth in the presented tumor models. M1043 is a mouse-specific endoglin-targeting antibody, which efficiently inhibits downstream BMP9-induced signaling (Supplementary Fig. S5; ref. 12), while TRC105 less effectively inhibits mouse BMP9 binding to endoglin. Rat IgG1 is, however, not capable of inducing ADCC, compared with other isotypes, making it an interesting approach to change the M1043 isotype to Mouse IgG2a, thereby creating an antibody which blocks ligand binding but also induces ADCC.

Fc-mediated effects have been clearly shown for human IgG subtypes and the human IgG1 antibody TRC105, which is able to bind mouse Fc receptors (28). Moreover, FcγR-mediated ADCC appeared crucial for the mechanism of action of endoglin antibody in our tumor models. In humans, the TRC105 IgG isotype may bind with higher affinity to Fc receptors compared with mouse Fc receptors, even further enhancing ADCC responses. Previous studies have shown that the therapeutic PD1 antibody effects are independent on Fc receptor binding (29). These data also indicate that evoking an immune response might be a more important mechanism of action for endoglin antibodies than inhibiting BMP9 binding.

In addition to endothelial cells, endoglin expression has been reported on (cancer associated) fibroblasts in prostate cancer (30) and colorectal cancer (3). Endoglin expression seems to be important for fibroblast survival *in vitro* and stimulates metastatic dissemination (3). Furthermore, endoglin expression has also been described on macrophages, where it seems to be important for differentiation and phagocytosis (31). In this study we show that endoglin is expressed by Tregs, posing them as a novel target for endoglin-targeted therapy. Although endoglin expression on $CD4^+$ cells has also been observed by others (32–34), endoglin expression on Treg cells has only been described before in an *in vitro* setting, in which Tregs were cultured with adipose-derived mesenchymal stromal cells (34). Strikingly, we observed that endoglin expression on Tregs is significantly increased in tumor tissue compared with the peripheral circulation. Furthermore, we show that endoglin-targeted therapy decreased the number of Tregs in tumors, thereby potentially contributing to the tumor responses. Depletion of Tregs within the tumor using antibody therapy has also been shown by others, for example using anti-CD25 (35) and anti-CTLA-4 antibodies (36) in mice. Because endoglin therapy targets multiple subsets of cells within the TME (i.e., proliferating endothelial cells, fibroblasts, and Tregs), TRC105 may more efficiently inhibit tumor growth and metastasis compared with other antiangiogenic therapies. The fact that endoglin-expressing Tregs could be detected in colorectal cancer tissue might explain the data from a previous clinical trial showing a significantly decreased number of circulating Tregs upon TRC105 therapy (18). Although, we could not show a clear endoglin-positive population in the blood of mice (**Fig. 5E**), we were able to detect endoglin-expressing Tregs in the blood of healthy volunteers (Supplementary Fig. S5D).

In conclusion, in this study we show that combining endoglin with PD1-targeted therapy in four preclinical cancer models strongly increases therapeutic effects. We propose a model in which TRC105 binds to endoglin-expressing endothelial cells, fibroblasts, and endoglin-expressing Tregs within the tumor, evoking an FcγR-dependent ADCC response. Consequently, the increased recruitment and activity of $CD8^+$ cells evokes sustained tumor regression and produce a memory T-cell response. Results from a phase Ib dose escalation study of carotuximab (TRC105) in combination with nivolumab (anti-PD1) in patients with metastatic non–small cell lung cancer (NCT03181308) should reveal whether this combination strategy is effective in human patients.

Disclosure of Potential Conflicts of Interest

A.B. Nixon is an employee/paid consultant for GlaxoSmithKline, Kanghong Pharma, Eli Lilly, and Promega, and reports receiving commercial research grants from TRACON Pharmaceuticals, Acceleron Pharma, and MedPacto, Inc. C.P. Theuer is an employee/paid consultant for TRACON Pharmaceuticals. L.J.A.C. Hawinkels reports receiving commercial research grants from TRACON Pharmaceuticals and is co-inventor on patent TRC105/PD1 combination (rights transferred to TRACON Pharmaceuticals). No potential conflicts of interest were disclosed by the other authors.

Authors' Contributions

Conception and design: M.J.A. Schoonderwoerd, J.C.H. Hardwick, C.P. Theuer, M.F. Fransen, L.J.A.C. Hawinkels
Development of methodology: M.J.A. Schoonderwoerd
Acquisition of data (provided animals, acquired and managed patients, provided facilities, etc.): M.J.A. Schoonderwoerd, M.F.M. Koops, R.A. Angela, B. Koolmoes, M. Paauwe, C.F.M. Sier
Analysis and interpretation of data (e.g., statistical analysis, biostatistics, computational analysis): M.J.A. Schoonderwoerd, M.F.M. Koops, R.A. Angela, B. Koolmoes, M.C. Barnhoorn, A.B. Nixon, M.F. Fransen, L.J.A.C. Hawinkels

Downloaded from http://aacrjournals.org/clincancerres/article-pdf/26/14/3831/2062840/3831.pdf by Leiden Uni - WALAEUS LIBRARY user on 01 September 2022

Writing, review, and/or revision of the manuscript: M.J.A. Schoonderwoerd, M.C. Barnhoorn, Y. Liu, C.F.M. Sier, J.C.H. Hardwick, A.B. Nixon, C.P. Theuer, M.F. Fransen, L.J.A.C. Hawinkels
Administrative, technical, or material support (i.e., reporting or organizing data, constructing databases): M.J.A. Schoonderwoerd, M.F.M. Koops, R.A. Angela, M. Toitou
Study supervision: M.J.A. Schoonderwoerd, J.C.H. Hardwick, M.F. Fransen, L.J.A.C. Hawinkels
Other (participated in some of the experimental procedures): M. Toitou

Acknowledgments

This study was supported by a sponsored research grant from TRACON Pharmaceuticals to both Duke and Leiden University Medical Center, and research grants from Stichting Fonds Oncologie Holland, and Stichting Sasha Swarttouw-Hijmans and Dutch Cancer Society (UL2014-6828). We would like to thank Dr. Sjef Verbeek for the FcγR I,II,III,IV KO mice and Kees Franken for the MC38-specific tetramers. Finally, the authors would like to thank the Animal facility of the Leiden University Medical Center and the Duke Preclinical Translational Research Unit for facilitating the mice experiments.

The costs of publication of this article were defrayed in part by the payment of page charges. This article must therefore be hereby marked *advertisement* in accordance with 18 U.S.C. Section 1734 solely to indicate this fact.

Received September 13, 2019; revised March 16, 2020; accepted April 21, 2020; published first April 24, 2020.

References

1. Saad RS, Liu YL, Nathan G, Celebrezze J, Medich D, Silverman JF. Endoglin (CD105) and vascular endothelial growth factor as prognostic markers in colorectal cancer. Mod Pathol 2004;17:197–203.
2. Zhang J, Zhang L, Lin Q, Ren W, Xu G. Prognostic value of endoglin-assessed microvessel density in cancer patients: a systematic review and meta-analysis. Oncotarget 2018;9:7660–71.
3. Paauwe M, Schoonderwoerd MJA, Helderman R, Harryvan TJ, Groenewoud A, van Pelt GW, et al. Endoglin expression on cancer-associated fibroblasts regulates invasion and stimulates colorectal cancer metastasis. Clin Cancer Res 2018;24:6331–44.
4. Lastres P, Bellon T, Cabanas C, Sanchez-Madrid F, Acevedo A, Gougos A, et al. Regulated expression on human macrophages of endoglin, an Arg-Gly-Asp-containing surface antigen. Eur J Immunol 1992;22:393–7.
5. O'Connell PJ, McKenzie A, Fisicaro N, Rockman SP, Pearse MJ, d'Apice AJ. Endoglin: a 180-kD endothelial cell and macrophage restricted differentiation molecule. Clin Exp Immunol 1992;90:154–9.
6. Takahashi N, Haba A, Matsuno F, Seon BK. Antiangiogenic therapy of established tumors in human skin/severe combined immunodeficiency mouse chimeras by anti-endoglin (CD105) monoclonal antibodies, and synergy between anti-endoglin antibody and cyclophosphamide. Cancer Res 2001;61:7846–54.
7. Tsujie M, Tsujie T, Toi H, Uneda S, Shiozaki K, Tsai H, et al. Anti-tumor activity of an anti-endoglin monoclonal antibody is enhanced in immunocompetent mice. Int J Cancer 2008;122:2266–73.
8. Matsuno F, Haruta Y, Kondo M, Tsai H, Barcos M, Seon BK. Induction of lasting complete regression of preformed distinct solid tumors by targeting the tumor vasculature using two new anti-endoglin monoclonal antibodies. Clin Cancer Res 1999;5:371–82.
9. Seon BK, Matsuno F, Haruta Y, Kondo M, Barcos M. Long-lasting complete inhibition of human solid tumors in SCID mice by targeting endothelial cells of tumor vasculature with antihuman endoglin immunotoxin. Clin Cancer Res 1997;3:1031–44.
10. Paauwe M, Heijkants RC, Oudt CH, van Pelt GW, Cui C, Theuer CP, et al. Endoglin targeting inhibits tumor angiogenesis and metastatic spread in breast cancer. Oncogene 2016;35:4069–79.
11. Seon BK, Haba A, Matsuno F, Takahashi N, Tsujie M, She X, et al. Endoglin-targeted cancer therapy. Curr Drug Deliv 2011;8:135–43.
12. Nolan-Stevaux O, Zhong W, Culp S, Shaffer K, Hoover J, Wickramasinghe D, et al. Endoglin requirement for BMP9 signaling in endothelial cells reveals new mechanism of action for selective anti-endoglin antibodies. PLoS One 2012;7:e50920.
13. Ishida Y, Agata Y, Shibahara K, Honjo T. Induced expression of PD-1, a novel member of the immunoglobulin gene superfamily, upon programmed cell death. EMBO J 1992;11:3887–95.
14. Kleinovink JW, Marijt KA, Schoonderwoerd MJA, van Hall T, Ossendorp F, Fransen MF. PD-L1 expression on malignant cells is no prerequisite for checkpoint therapy. Oncoimmunology 2017;6:e1294299.
15. Robert C, Ribas A, Wolchok JD, Hodi FS, Hamid O, Kefford R, et al. Anti-programmed-death-receptor-1 treatment with pembrolizumab in ipilimumab-refractory advanced melanoma: a randomised dose-comparison cohort of a phase 1 trial. Lancet 2014;384:1109–17.
16. Garon EB, Rizvi NA, Hui R, Leighl N, Balmanoukian AS, Eder JP, et al. Pembrolizumab for the treatment of non-small-cell lung cancer. N Engl J Med 2015;372:2018–28.
17. Motzer RJ, Rini BI, McDermott DF, Redman BG, Kuzel TM, Harrison MR, et al. Nivolumab for metastatic renal cell carcinoma: results of a randomized phase II trial. J Clin Oncol 2015;33:1430–7.
18. Karzai FH, Apolo AB, Cao L, Madan RA, Adelberg DE, Parnes H, et al. A phase I study of TRC105 anti-endoglin (CD105) antibody in metastatic castration-resistant prostate cancer. BJU Int 2015;116:546–55.
19. Fransen MF, Benonisson H, van Maren WW, Sow HS, Breukel C, Linssen MM, et al. A restricted role for FcγR in the regulation of adaptive immunity. J Immunol 2018;200:2615–26.
20. Hand PH, Robbins PF, Salgaller ML, Poole DJ, Schlom J. Evaluation of human carcinoembryonic-antigen (CEA)-transduced and non-transduced murine tumors as potential targets for anti-CEA therapies. Cancer Immunol Immunother 1993;36:65–75.
21. Tseng W, Leong X, Engleman E. Orthotopic mouse model of colorectal cancer. J Vis Exp 2007;10:484.
22. De Robertis M, Massi E, Poeta ML, Carotti S, Morini S, Cecchetelli L, et al. The AOM/DSS murine model for the study of colon carcinogenesis: from pathways to diagnosis and therapy studies. J Carcinog 2011;10:9.
23. Yadav M, Jhunjhunwala S, Phung QT, Lupardus P, Tanguay J, Bumbaca S, et al. Predicting immunogenic tumour mutations by combining mass spectrometry and exome sequencing. Nature 2014;515:572–6.
24. Tabata M, Kondo M, Haruta Y, Seon BK. Antiangiogenic radioimmunotherapy of human solid tumors in SCID mice using (125)I-labeled anti-endoglin monoclonal antibodies. Int J Cancer 1999;82:737–42.
25. Liu Z, Lebrin F, Maring JA, van den Driesche S, van der Brink S, van Dinther M, et al. ENDOGLIN is dispensable for vasculogenesis, but required for vascular endothelial growth factor-induced angiogenesis. PLoS One 2014;9:e86273.
26. Liu Y, Starr MD, Brady JC, Dellinger A, Pang H, Adams B, et al. Modulation of circulating protein biomarkers following TRC105 (anti-endoglin antibody) treatment in patients with advanced cancer. Cancer Med 2014;3:580–91.
27. Liu Y, Starr MD, Brady JC, Rushing C, Pang H, Adams B, et al. Modulation of circulating protein biomarkers in cancer patients receiving bevacizumab and the anti-endoglin antibody, TRC105. Mol Cancer Ther 2018;17:2248–56.
28. Dekkers G, Bentlage AEH, Stegmann TC, Howie HL, Lissenberg-Thunnissen S, Zimring J, et al. Affinity of human IgG subclasses to mouse Fc gamma receptors. MAbs 2017;9:767–73.
29. Dahan R, Sega E, Engelhardt J, Selby M, Korman AJ, Ravetch JV. FcγRs modulate the anti-tumor activity of antibodies targeting the PD-1/PD-L1 axis. Cancer Cell 2015;28:543.
30. Romero D, O'Neill C, Terzic A, Contois L, Young K, Conley BA, et al. Endoglin regulates cancer-stromal cell interactions in prostate tumors. Cancer Res 2011;71:3482–93.
31. Ojeda-Fernandez L, Recio-Poveda L, Aristorena M, Lastres P, Blanco FJ, Sanz-Rodriguez F, et al. Mice lacking endoglin in macrophages show an impaired immune response. PLoS Genet 2016;12:e1005935.
32. Nowaczyk RM, Jursza-Piotrowska E, Gram A, Siemieniuch MJ, Boos A, Kowalewski MP. Cells expressing CD4, CD8, MHCII and endoglin in the canine corpus luteum of pregnancy, and prepartum activation of the luteal TNFα system. Theriogenology 2017;98:123–32.
33. Schmidt-Weber CB, Letarte M, Kunzmann S, Ruckert B, Bernabeu C, Blaser K. TGF-{beta} signaling of human T cells is modulated by the ancillary TGF-{beta} receptor endoglin. Int Immunol 2005;17:921–30.

Downloaded from http://aacrjournals.org/clincancerres/article-pdf/26/14/3831/2062840/3831.pdf by Leiden Uni - WALAEUS LIBRARY user on 01 September 2022

34. Quaedackers ME, Baan CC, Weimar W, Hoogduijn MJ. Cell contact interaction between adipose-derived stromal cells and allo-activated T lymphocytes. Eur J Immunol 2009;39:3436–46.
35. Arce Vargas F, Furness AJS, Solomon I, Joshi K, Mekkaoui L, Lesko MH, et al. Fc-Optimized anti-CD25 depletes tumor-infiltrating regulatory T cells and synergizes with PD-1 blockade to eradicate established tumors. Immunity 2017;46:577–86.
36. Tang F, Du X, Liu M, Zheng P, Liu Y. Anti-CTLA-4 antibodies in cancer immunotherapy: selective depletion of intratumoral regulatory T cells or checkpoint blockade? Cell Biosci 2018;8:30.

Downloaded from http://aacrjournals.org/clincancerres/article-pdf/26/14/3831/2062840/3831.pdf by Leiden Uni - WALAEUS LIBRARY user on 01 September 2022